Aggravated effects of human parvovirus B19 NS1 protein on bleomycin-induced pulmonary fibrosis

TSAI-CHING HSU[1-3], CHIH-CHEN TZANG[4], CHIA-WEI KUO[1], ZHI-HAN WEN[1], DER-YUAN CHEN[1,5-7] and BOR-SHOW TZANG[1-3,8]

[1]Institute of Medicine, Chung Shan Medical University, Taichung 402, Taiwan, R.O.C.; [2]Department of Clinical Laboratory, Chung Shan Medical University Hospital, Taichung 402, Taiwan, R.O.C.; [3]Immunology Research Center, Chung Shan Medical University, Taichung 402, Taiwan, R.O.C.; [4]School of Medicine, College of Medicine, National Taiwan University, Taipei City 100, Taiwan, R.O.C.; [5]College of Medicine, China Medical University, Taichung 404, Taiwan, R.O.C.; [6]Rheumatology and Immunology Center, China Medical University Hospital, Taichung 404, Taiwan, R.O.C. [7]Translational Medicine Laboratory, Rheumatology and Immunology Center, China Medical University Hospital, Taichung 404, Taiwan, R.O.C.; [8]Department of Biochemistry, School of Medicine, Chung Shan Medical University, Taichung 402, Taiwan, R.O.C.

Received September 13, 2025; Accepted November 27, 2025

DOI: 10.3892/mmr.2025.13779

Abstract. Interstitial lung diseases (ILDs) include various lung parenchymal disorders characterized by inflammation and fibrosis of the lung tissue, leading to progressive dyspnea and respiratory failure. Clinical evidence has suggested an association between human parvovirus B19 (B19V) infection and the progression of ILD and pulmonary fibrosis, but the mechanisms involved remain unclear. The present study screened 86 patients with connective tissue disease (CTD) and reported that B19V infection was significantly more prevalent among those with ILD than among those without (P<0.001). To investigate the potential underlying mechanisms, a bleomycin (BLM)-treated mouse model was employed to assess the effect of B19V nonstructural protein 1 (NS1) on pulmonary fibrosis. Mice treated with BLM or BLM + NS1 exhibited markedly higher fibrosis scores, hydroxyproline content, and higher levels of transforming growth factor-β and collagen I. Treatment with nintedanib attenuated fibrosis in both groups; however, lung fibrosis remained more pronounced in the BLM + NS1 group than in the BLM group. Furthermore, the levels of neutrophil-associated markers, including citrullinated histone H3 and myeloperoxidase, as well as inflammasome-related factors, such as IL-18 and IL-17A, were markedly elevated in lung tissues from both groups, with the highest levels observed in the BLM + NS1 group. These findings suggested that B19-NS1 may exacerbate fibrosis in patients with ILD by increasing neutrophil-driven responses and inflammasome activation, highlighting a need for nintedanib therapies to more effectively address B19V-associated pulmonary fibrosis.

Correspondence to: Dr Der-Yuan Chen, Rheumatology and Immunology Center, China Medical University Hospital, 2 Yude Road, North, Taichung 404, Taiwan, R.O.C.
E-mail: dychen1957@gmail.com

Dr Bor-Show Tzang, Department of Biochemistry, School of Medicine, College of Medicine, Chung Shan Medical University, 110 Sec. 1 Jianguo N. Road, Taichung 402, Taiwan, R.O.C.
E-mail: bstzang@csmu.edu.tw

Key words: interstitial lung diseases, parvovirus B19, nonstructural protein 1, pulmonary fibrosis, bleomycin, nintedanib

Introduction

Interstitial lung disease (ILD), a heterogeneous pulmonary parenchymal disease, is a major cause of pulmonary fibrosis characterized by inflammation and fibrosis of the lung parenchyma (1). The etiology of most ILDs remains unknown, with idiopathic pulmonary fibrosis (IPF) being the most common and characterized by progressive lung tissue hardening, breathing difficulties, and eventual respiratory failure (2). Known ILDs include connective tissue disease (CTD)-ILD, which is more likely to develop into progressive fibrosing ILD (PF-ILD), particularly in patients with conditions such as rheumatoid arthritis (RA), systemic lupus erythematosus, polymyositis and dermatomyositis, with PF-ILD progression rates as high as 20% (3,4). Fibrosis is primarily caused by the activation of fibroblasts, which is triggered by chronic injury or inflammation, resulting in cell destruction and abnormal tissue repair. Fibroblasts migrate to injury sites, release growth factors and profibrotic mediators, and transform into myofibroblasts that secrete excessive amounts of extracellular matrix, causing tissue stiffness and progressive interstitial pneumonia (5,6). All PF-ILDs are triggered by chronic epithelial or vascular injury or granulomatous inflammation, leading to abnormal repair processes and ultimately causing fibrosis (5,6).

Human parvovirus B19 (B19V), a member of the *Erythrovirus* genus within the Parvoviridae family, is a small, non-enveloped virus with a linear, single-stranded DNA genome (7). The capsid of B19V is a stable icosahedral structure composed mainly of viral protein (VP) 1 and VP2

proteins. VP1 and VP2 are identical except for a unique 227-amino-acid region at the N-terminus of VP1 (VP1u) (8). The unique VP1 region (VP1u) of B19V plays roles in viral tropism, uptake, and nuclear entry. It contains a nuclear localization signal, targets erythroid progenitor cells, and is targeted by neutralizing antibodies (8). The nonstructural protein (NS)-1 of B19V is essential for viral DNA replication and gene regulation. B19V NS1 contains nuclear localization signals, a DNA-binding/nuclease domain, an ATPase and NTP-binding motif, and a transactivation domain (7,8). B19V NS1 can transactivate host genes, induce apoptosis, cause cell cycle arrest, and elicit inflammatory cytokines and DNA damage responses (7,8).

Although most individuals infected with B19V are asymptomatic or present with mild, nonspecific symptoms resembling those of the common cold (7-9), accumulating evidence has linked B19V to the pathogenesis of ILDs (10-12). B19V has been associated with chronic vasculopathy syndromes, including Wegener's granulomatosis, dermatomyositis, and scleroderma (13-15) and has been implicated in the progression of IPF through the induction of endothelial immunogenicity (16). Case reports and clinical studies have identified B19V DNA in lung biopsies and BALF from ILD patients (11,17) and morphological evidence of septal capillary injury has been observed in ILD case series with chronic B19V infection (18).

Despite this, the mechanisms underlying the role of B19V in ILD remain unclear. Prior studies have shown that B19V NS1 can transactivate expression of the IL-6 gene (19,20), a cytokine recognized as a key mediator and biomarker of lung fibrosis (21,22). An *in vitro* study demonstrated that B19V can also activate human dermal fibroblasts, indicating its role in fibrosis and systemic sclerosis (23). Given the antifibrotic effects of nintedanib in patients with CTD-ILD, the present study was conducted to elucidate the effect of B19V NS1 on pulmonary fibrosis using a bleomycin (BLM)-treated mouse model and to evaluate the therapeutic effect of nintedanib, thereby clarifying the mechanistic association between B19V infection and ILD in CTD patients.

Materials and methods

Human samples of CTD patients. A total of 86 patients diagnosed with CTD (19 males and 67 females, aged 34-84 years) with or without ILD according to the clinical criteria (24) were recruited between November 1, 2021 and October 31, 2024, at the Rheumatology and Immunology Center of the China Medical University Hospital, Taichung, Taiwan. The China Medical University Hospital's Institutional Review Board approved the current study (IRB approval no. CMUH110-REC2-178) and all participants provided written informed consent following the Declaration of Helsinki's ethical guidelines for medical research involving human subjects. Peripheral blood samples (10 ml) were collected into glass tubes containing no additive or anticoagulant. The clotted blood samples were centrifuged at 2,000 x g for 10 min at 4˚C, and the sera were collected and stored at -80˚C until use. Human parvovirus B19 infection was determined using parvovirus B19V IgM and IgG ELISA kits (cat. nos. IB79807 and IB79806; IBL-America), and Cytomegalovirus (CMV) infection was determined using CMV IgM and IgG test system (ZEUS Scientific, Inc.) from serum samples according to the manufacturer's instructions. COVID-19 infection was determined using the cobas SARS-CoV-2 RT-PCR test (Roche Molecular Diagnostics) from nasopharyngeal swab samples. Herpes zoster was determined to be caused by a varicella-zoster virus infection, as indicated by the presence of the virus in blood or urine samples.

Animals and treatments. A total of 25 male C57BL/6 mice (age, 6 weeks; weight, 17-19 g) were obtained from the National Laboratory Animal Center and housed at Chung Shan Medical University under controlled lighting (12-h light/dark cycle), temperature (22-24˚C) and humidity (50-60%) conditions, with free access to water and standard laboratory chow (Lab Diet 5001; PMI Nutrition International Inc.). The experimental protocols were approved by the Institutional Animal Care and Use Committee, Chung Shan Medical University, Taiwan (IACUC approval nos. 2803 and 112065). Based on a previous publication, a BLM-induced lung fibrosis mouse model was performed (25). Bleomycin, commonly administered intratracheally in mice, is widely used for pulmonary fibrosis models due to its ability to induce cellular damage and fibrosis (2,26). The present study employed the intratracheal administration route. At eight weeks of age, the mice were randomly divided into five groups (n=5 per group): i) Control (PBS) group; ii) Bleomycin (BLM) group; iii) BLM + nintedanib group; iv) BLM + NS1 group; and v) BLM + NS1 + nintedanib group. The Control and BLM groups received intratracheal PBS and intratracheal BLM (3 mg/kg) on day 0, respectively. The BLM + nintedanib group received intratracheal BLM on day 0 and nintedanib (50 mg/kg) intraperitoneally every 2 days, starting from day 10, for a total of 5 injections (27). The BLM + NS1 group received intratracheal BLM (3 mg/kg) and B19V-NS1 recombinant protein (0.8 mg/kg) on day 0. The BLM + NS1 + nintedanib group received intratracheal BLM (3 mg/kg) and B19V-NS1 recombinant protein (0.8 mg/kg) on day 0. nintedanib (50 mg/kg) was administered intraperitoneally every 2 days, starting from day 10, for a total of 5 injections. On day 19, the mice were sacrificed using a carbon dioxide (CO_2) euthanasia chamber. The CO_2 flow rate was 50% of the chamber volume/min. After visually confirming that the mice had stopped breathing, the CO_2 flow was maintained for an additional minute to ensure mortality. Then, bronchoalveolar lavage fluid (BALF) and lung tissues were collected.

Hydroxyproline analysis. Lung tissues were processed and hydrolyzed according to the manufacturer's instructions using a Hydroxyproline Assay Kit (ab222941, Abcam). After homogenization, hydrolysis, and neutralization, samples were centrifuged at 10,000 x g for 5 min at 4˚C and dried. The hydroxyproline standard curve was generated, and absorbance was measured at 560 nm using a SpectraMax M5 Microplate Reader (Molecular Devices LLC).

BALF. The collection of BALF was performed as described previously (28). Briefly, mice were sacrificed and 1 ml of PBS was injected into the trachea and aspirated three times. The collected lavage fluid was centrifuged at 200 x g for 10 min at 4˚C, and the supernatant was reserved for ELISA analysis. Additionally, the cell pellet was re-suspended in 150 μl of

PBS, and the cell populations were detected using a cytospin to prepare the slides, which were then stained with Liu's stain (Liu's A for 30 sec and Liu's B for 90 sec at room temperature) for microscopic observation and enumeration of macrophages, neutrophils, and lymphocytes.

ELISA. A total of 100 μl BALF samples was added to the ELISA plate wells and incubated at 37˚C for 90 min. After washing, a biotinylated antibody (100 μl) was added and incubated for 60 min at the same temperature. The wells were then washed, and 100 μl enzyme conjugate was added for a 30-min incubation. Subsequently, substrate (100 μl) was added and incubated in the dark at 37˚C after washing thoroughly. The quantification of essential ILD biomarkers, including interleukin (IL)-6, tumor necrosis factor (TNF)-α, and Krebs von den Lungen (KL)-6 (29,30), was performed by duplicating ELISA kits for mouse IL-6, TNF-α (Invitrogen; Thermo Fisher Scientific, Inc.), and KL-6 (MyBioSource, Inc.), following the manufacturer's protocol. Absorbance was measured at 450 nm.

Histological analysis. Histological evaluation of lung tissues was performed with paraffin sections undergoing hematoxylin and eosin (H&E) staining and Masson's trichrome staining. For H&E staining, the tissues were immersed in 10% formalin at 25˚C for 24 h and then embedded in paraffin. The tissue blocks were sliced into 5-μm sections, deparaffinized using xylene, and dehydrated by passing through decreasing concentrations of ethanol (100, 90, 80 and 70%) and water. Subsequently, the slides were stained with hematoxylin for 3 min at 25˚C, rinsed with water and stained with eosin for 5 min at 25˚C. Each slide was subsequently immersed in 95 and 100% ethanol twice (1 min each immersion). Finally, the slides were immersed in xylene twice for 2 min and then air-dried. For Masson's trichrome staining, sections were deparaffinized, rehydrated, and incubated in Bouin's fluid at 60˚C for 60 min. They were stained with Weigert's hematoxylin for 2 min at 25˚C, Biebrich scarlet/acid fuchsin for 10 min and aniline blue for 10 min at 25˚C. Finally, sections were treated with 1% acetic acid, dehydrated, cleared, and mounted, with collagen fibers staining blue, muscle fibers red, cytoplasm pink and nuclei dark brown or black. Photomicrographs were observed using TissueFAX Plus (TissueGnostics GmbH) to analyze stained sections. A total of five 100-μm fields of view were examined in each section. The fibrosis score was evaluated and graded using the modified Ashcroft score (31). Grade 0 signified normal lung tissue without fibrosis, and grades 1-8 represent varying levels of fibrosis from minor to serious.

Immunohistochemistry (IHC). The aforementioned paraffin-embedded sections (5 μm) were fixed in acetone for 5 min at 25˚C, air-dried for 10 min, and then immersed in 0.3% H_2O_2/PBS for 5 min at 25˚C to block peroxidase activity and blocked with 3% BSA (Sigma-Aldrich; Merck KGaA) in PBS + 0.05% Tween 20 (PBS-Tween) for 1 h at 25˚C. After washing twice with PBS-Tween, each for 10 min, antibodies against transforming growth factor (TGF)-β (1:100; cat. no. A16640; ABclonal Biotech Co., Ltd.), collagen I (1:100; cat. no. A5786; ABclonal Biotech Co., Ltd.), IL-18 (1:200; cat. no. A23076; ABclonal Biotech Co., Ltd.), IL-17A (1:200; cat. no. A12454; ABclonal Biotech Co., Ltd.), citrullinated histone H3 (Cit-H3; (1:100; cat no. ab5103; Abcam) and myeloperoxidase (MPO; 1:500; cat. no. ab208670; Abcam) were applied and incubated for 1 h, followed by incubation with horseradish peroxidase (HRP)-labeled secondary antibodies (1:5,000; cat. no. sc-2004; Santa Cruz Biotechnology, Inc.) for 1 h. Sections were developed with DAB for 3 min, then washed with distilled water for an additional 5 min. Subsequently, hematoxylin was used as a counterstain for 3 min at 25˚C and the sections were washed with distilled water for 10 min. The sections were then dehydrated using a graded ethanol series (80, 95 and 100%; 5 min each), followed by immersion in xylene twice for 5 min each and air-drying. A tissue quantification analyzer (TissueFAX Plus; TissueGnostics GmbH) was used to analyze stained sections, counting positive cells in randomly selected fields and comparing the results with those of a negative control. A total of five 100 μm fields of view were examined in each section, across five fields of view counted and averaged.

Statistical analysis. Data were recorded and analyzed using Excel (Microsoft Corporation) and GraphPad Prism 8.0 (Dotmatics) software. Experimental results are presented as mean ± SD, and statistical significance was determined using one-way ANOVA with Tukey's multiple comparisons post hoc test. Fibrosis score results were presented as medians and ranges and were analyzed using one-way ANOVA with the Kruskal-Wallis test and Dunn's post hoc test. BALF cell counts were analyzed using two-way ANOVA with Tukey's multiple comparisons post hoc test, and the χ^2 test was used to determine the significant differences in clinical characteristics between the data sets. $P<0.05$ was considered statistically significant.

Results

Prevalence of B19V infection in CTD patients. As illustrated in Table I, B19V infection (24/33 vs. 12/53; $P<0.001$) and hypertension (14/33 vs. 11/53; $P=0.03$) were significantly more prevalent in CTD patients with ILD than in those without ILD. By contrast, no significant differences were detected in age at study entry, sex distribution, smoking status, disease duration, CMV, COVID-19, herpes zoster infection, or diabetes mellitus or cardiovascular disease status between the two groups. In terms of CTD type, among the 53 CTD patients without ILD, 50 had RA, one had idiopathic inflammatory myopathy (IIM), and two had systemic sclerosis (SSc). Among the 33 CTD patients with ILD, 25 had RA, five had IIM, and three had SSc. Additionally, the ILD subtypes included 26 cases of nonspecific interstitial pneumonia, five cases of usual interstitial pneumonia (UIP), and two cases of organizing pneumonia (OP).

Influence of B19V NS1 on body weights, lung weights, and survival rate in mice with BLM-induced pulmonary fibrosis. To assess the effects of B19V NS1 on BLM-induced pulmonary fibrosis, the body weights of the mice were recorded daily until day 19. By contrast, lung weights were measured on day 19 (Fig. 1A). Compared with those of the control group, the body weights of the mice in the BLM, BLM + nintedanib,

Table I. Clinical characteristics of 86 CTD patients with or without ILD.

Clinical characteristic	CTD without ILD (n=53)	CTD with ILD (n=33)	P-value
Age, years (mean ± SD) [range]	56.2±8.6 [34-75]	61.8±9.9 [36-84]	
Female (n=67)	43	24	0.36
Smoking (n=12)	7	5	0.80
B19V IgM or IgG (+) (n=36)	12	24	<0.001[a]
CMV IgM or IgG (+) (n=67)	41	26	0.84
COVID-19 (+) (n=33)	19	14	0.54
Herpes zoster (n=19)	15	4	0.08
CTD duration, years	9.6±2.7	10.7±2.6	
CTD types			
RA	50	25	
IIM	1	5	
SSc	2	3	
ILD patterns by HRCT			
NSIP	NA	26	NA
UIP	NA	5	NA
OP	NA	2	NA
Hypertension (n=25)	11	14	0.03[a]
DM (n=8)	3	5	0.14
CVD (n=9)	4	5	0.26

[a]P<0.05, vs. CTD patients without ILD, determined by the χ^2 test. CTD, connective tissue disease; ILD, interstitial lung disease; CMV, cytomegalovirus; ILD, interstitial lung disease; B19V, human parvovirus B19; RA, rheumatoid arthritis; IIM, idiopathic inflammatory myopathies; SSc, systemic sclerosis; HRCT, high-resolution computed tomography; NSIP, non-specificinterstitial pneumonia; UIP, usual interstitial pneumonia; OP, organizing pneumonitis; HT, hypertension; DM, diabetes mellitus; CVD, cardiovascular disease; NA, not applicable.

BLM + NS1, and BLM + NS1 + nintedanib groups significantly decreased (Fig. 1B; P=0.008, 0.002, <0.001 and <0.001, respectively). Treatment with nintedanib improved body weight loss in mice from both the BLM and the BLM + NS1 groups but was not sufficient to restore normal weight (Fig. 1B). Compared with the mice in the PBS group, the mice in the BLM and BLM + NS1 groups had significantly greater lung weights (P=0.025 and 0.037, respectively), whereas normal lung weight was restored in the nintedanib treatment groups (Fig. 1C; BLM + nintedanib vs. BLM, P=0.035; BLM + NS1 + nintedanib vs. BLM + NS1, P=0.044).

B19V NS1 administration changes immune cell compositions and increases levels of fibrotic markers in the BALF of mice with BLM-induced pulmonary fibrosis. To evaluate the influence of B19V NS1 on immune cell distribution in the BALF of mice treated with BLM, the proportions of macrophages, neutrophils and lymphocytes were analyzed. No significant difference in lymphocyte proportion was observed among the groups (Fig. 2A). Treatment with BLM resulted in a significant increase in the numbers of macrophages and neutrophils. Treatment with nintedanib partially reversed this trend by increasing the number of macrophages and reducing the number of neutrophils. Notably, the proportions of neutrophils remained elevated in the BLM + NS1 + nintedanib group, indicating that the NS1-induced effects were not fully mitigated by nintedanib (Fig. 2A; macrophages: BLM vs. PBS, P<0.001; BLM + nintedanib vs. PBS, P<0.001; BLM + NS1 vs. PBS, P=0.02; BLM + nintedanib + NS1 vs. PBS, P=0.005; BLM + NS1 vs. BLM, P<0.001; neutrophils: BLM vs. PBS, P<0.001; BLM + nintedanib vs. PBS, P<0.001; BLM + NS1 vs. PBS, P<0.001; BLM + nintedanib + NS1 vs. PBS, P<0.001; and BLM + NS1 vs. BLM, P=0.006). Additionally, an ELISA was performed to measure the levels of lung fibrosis-related markers, including TNF-α, KL-6, and IL-6, in the BALF. Compared with those in the control group (PBS), TNF-α (Fig. 2B; P=0.014 and 0.003, respectively), KL-6 (Fig. 2C; P<0.001 and P<0.001, respectively) and IL-6 (Fig. 2D; P=0.039 and 0.009, respectively) levels in the BALF of mice from the BLM and BLM + NS1 groups were markedly elevated. nintedanib treatment significantly reduced the expression of these markers in the BALF of mice from both the BLM and BLM + NS1 groups (Fig. 2B-D; TNF-α, BLM + nintedanib vs. BLM, P=0.039; BLM + NS1 + nintedanib vs. BLM + NS1, P=0.009; KL-6, BLM + nintedanib vs. BLM, P<0.001; BLM + NS1 + nintedanib vs. BLM + NS1, P<0.001; IL-6, BLM + nintedanib vs. BLM, P=0.013; BLM + NS1 + nintedanib vs. BLM + NS1, P=0.014).

B19V NS1 administration increases the lung fibrosis score and hydroxyproline content in mice with BLM-induced pulmonary fibrosis. Histological analyses were also performed to assess the effect of B19V NS1 on BLM-induced pulmonary fibrosis in mice. Significantly higher fibrosis scores were observed in

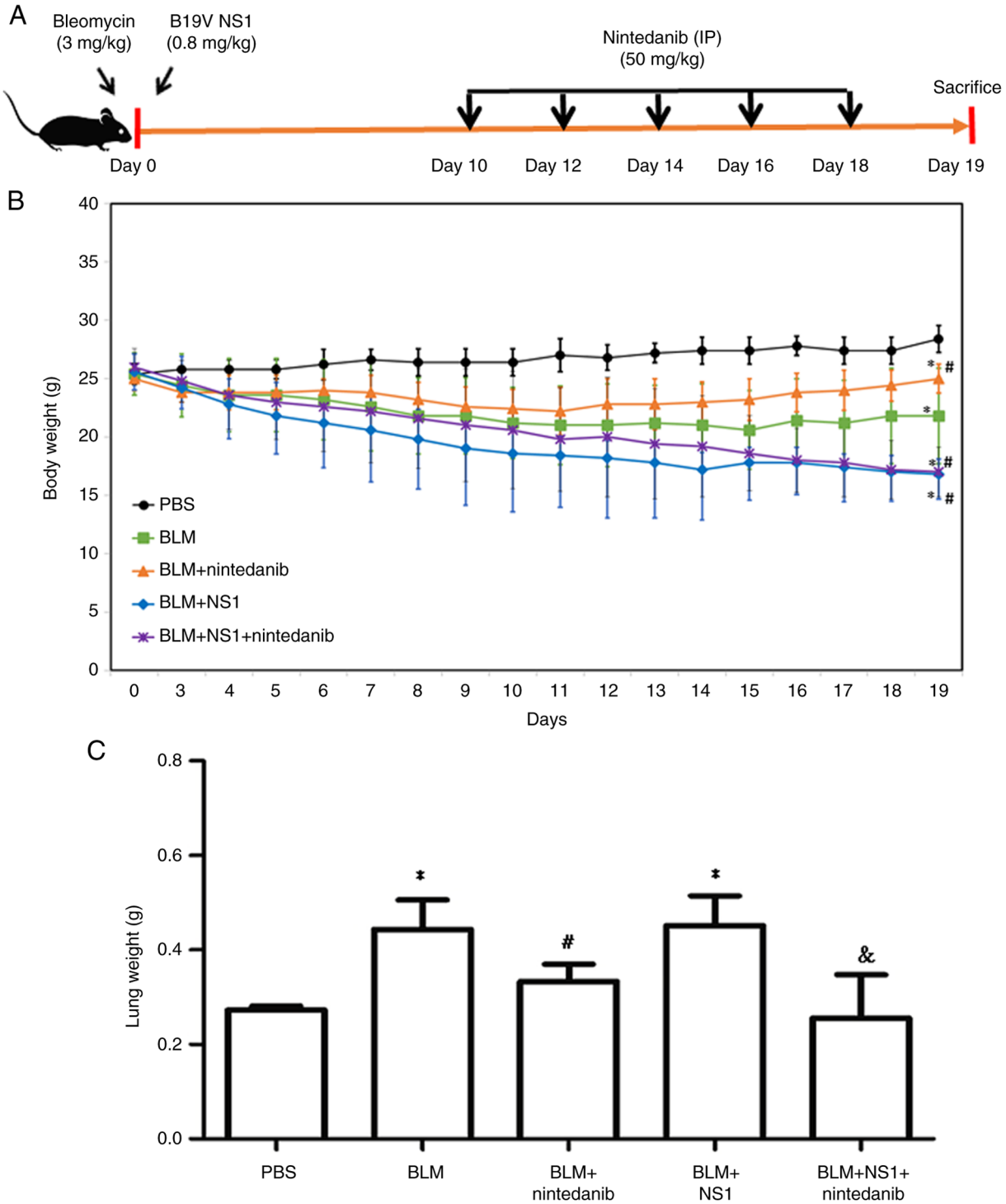

Figure 1. Effects of nintedanib and B19V NS1 on bleomycin-induced pulmonary fibrosis in mice. (A) Schematic diagram of the experimental animal model. (B) Daily body weight measurements across the PBS, BLM, BLM + nintedanib, BLM + NS1, and BLM + NS1 + nintedanib groups (BLM vs. PBS, P=0.008; BLM + nintedanib vs. PBS, P=0.002; BLM + NS1 vs. PBS, P<0.001; BLM + nintedanib + NS1 vs. PBS, P<0.001; BLM + NS1 vs. BLM, P=0.031; BLM + nintedanib + NS1 vs. BLM, P=0.048; BLM + nintedanib + NS1 vs. BLM + nintedanib, P<0.001). (C) Lung weight of mice on day 19 (BLM vs. PBS, P=0.025; BLM + NS1 vs. PBS, P=0.037; BLM + nintedanib vs BLM, P=0.035; BLM + NS1 + nintedanib vs BLM + NS1, P=0.044). *P<0.05 vs. the PBS (Control) group, #P<0.05 vs. the BLM group, and &P<0.05 vs. the BLM + NS1 group. B19V, human parvovirus B19; NS1, nonstructural protein 1; BLM, bleomycin.

the lungs of mice from the BLM and BLM + NS1 groups than in those from the PBS group (P<0.05 and P<0.001, respectively). Nintedanib reduced fibrosis levels in both the BLM + nintedanib group [3 (3-4)] and the BLM + NS1 + nintedanib group [4 (4-5)] (Fig. 3A-B). However, the lung fibrosis score remained more severe in the mice from the BLM + NS1 group [7 (7-8)] than in those from the BLM group [6 (5-7)] (Fig. 3B). Similarly, lung hydroxyproline content, an indicator of collagen deposition, was significantly greater in the lungs of mice from the BLM and BLM + NS1 groups than in those from the PBS group (P<0.001 and P<0.001, respectively). Hydroxyproline levels remained higher in the mice in the BLM + NS1 group

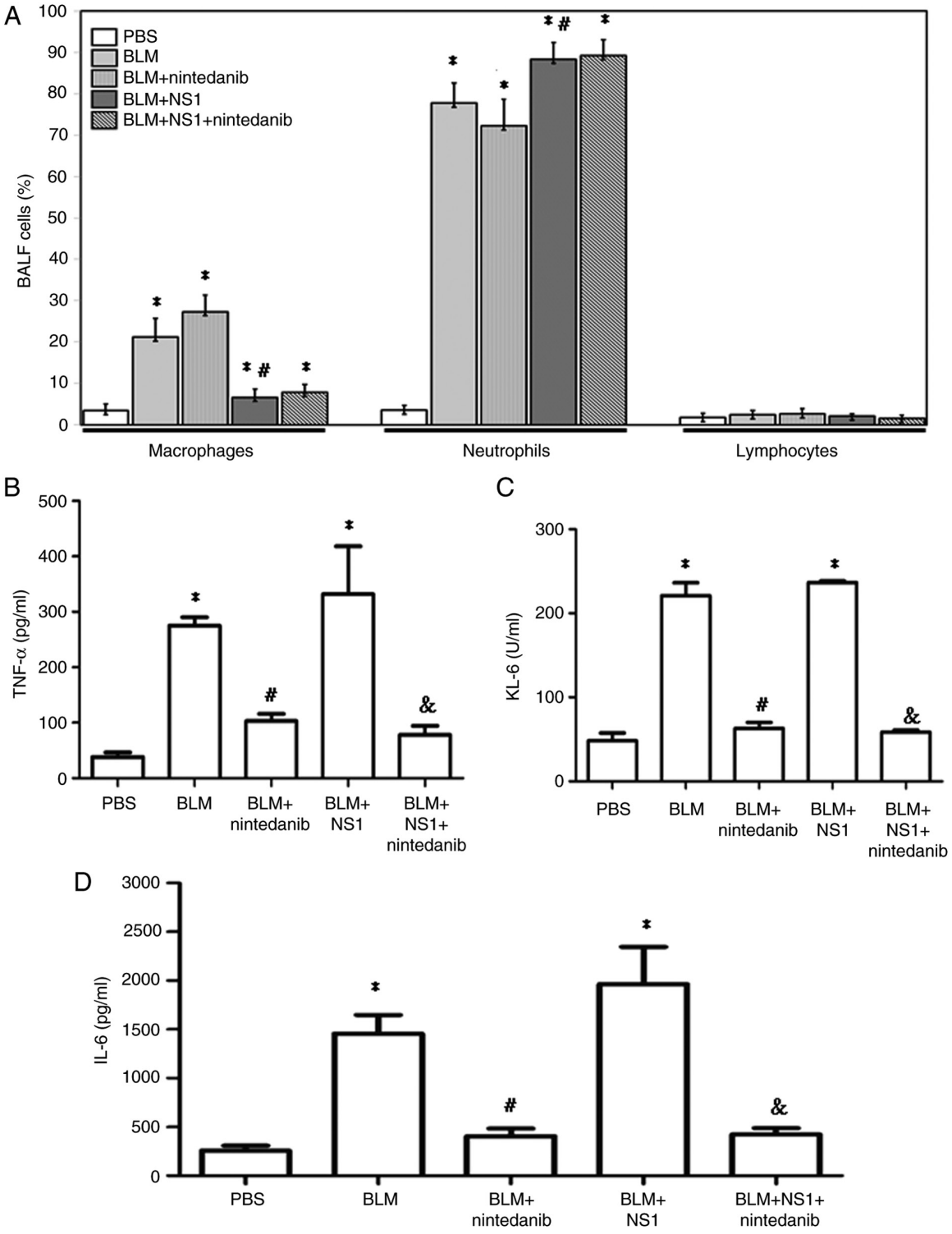

Figure 2. Proportions of immune cells in BALF of mice. (A) Percentages of macrophage, neutrophil, and lymphocyte in BALF of mice from different groups (Macrophages: BLM vs. PBS, P<0.001; BLM + nintedanib vs. PBS, P<0.001; BLM + NS1 vs. PBS, P=0.02; BLM + nintedanib + NS1 vs. PBS, P=0.005; BLM + NS1 vs. BLM, P<0.001; Neutrophils: BLM vs. PBS, P<0.001; BLM + nintedanib vs. PBS, P<0.001; BLM + NS1 vs. PBS, P<0.001; BLM + nintedanib + NS1 vs. PBS, P<0.001; BLM + NS1 vs. BLM, P=0.01). The concentrations of (B) TNF-α (BLM vs. PBS, P=0.014; BLM + NS1 vs. PBS, P=0.003; BLM + nintedanib vs. BLM, P=0.039; BLM + nintedanib + NS1 vs. BLM + NS1 P=0.009), (C) KL-6 (BLM vs. PBS, P<0.001; BLM + NS1 vs. PBS, P<0.001; BLM + nintedanib vs. BLM, P<0.001; BLM + nintedanib + NS1 vs. BLM + NS1 P<0.001) and (D) IL-6 (BLM vs. PBS, P= 0.039; BLM + NS1 vs. PBS, P=0.009; BLM + nintedanib vs. BLM, P=0.013; BLM + nintedanib + NS1 vs. BLM + NS1, P=0.014) in BALF of mice from different groups. *P<0.05 vs. the PBS (Control) group, #P<0.05 vs. the BLM group, and &P<0.05 vs. the BLM + NS1 group. BALF, bronchoalveolar lavage fluid; BLM, bleomycin; NS1, nonstructural protein 1; IL, interleukin.

than in the mice in the BLM group (P=0.016). Nintedanib treatment markedly reduced hydroxyproline levels, although the reduction was more pronounced in the BLM group and the BLM + NS1 group (P=0.004 and P=0.036, respectively) (Fig. 3C). Notably, significantly higher hydroxyproline levels were detected in the BLM + NS1 + nintedanib group than in

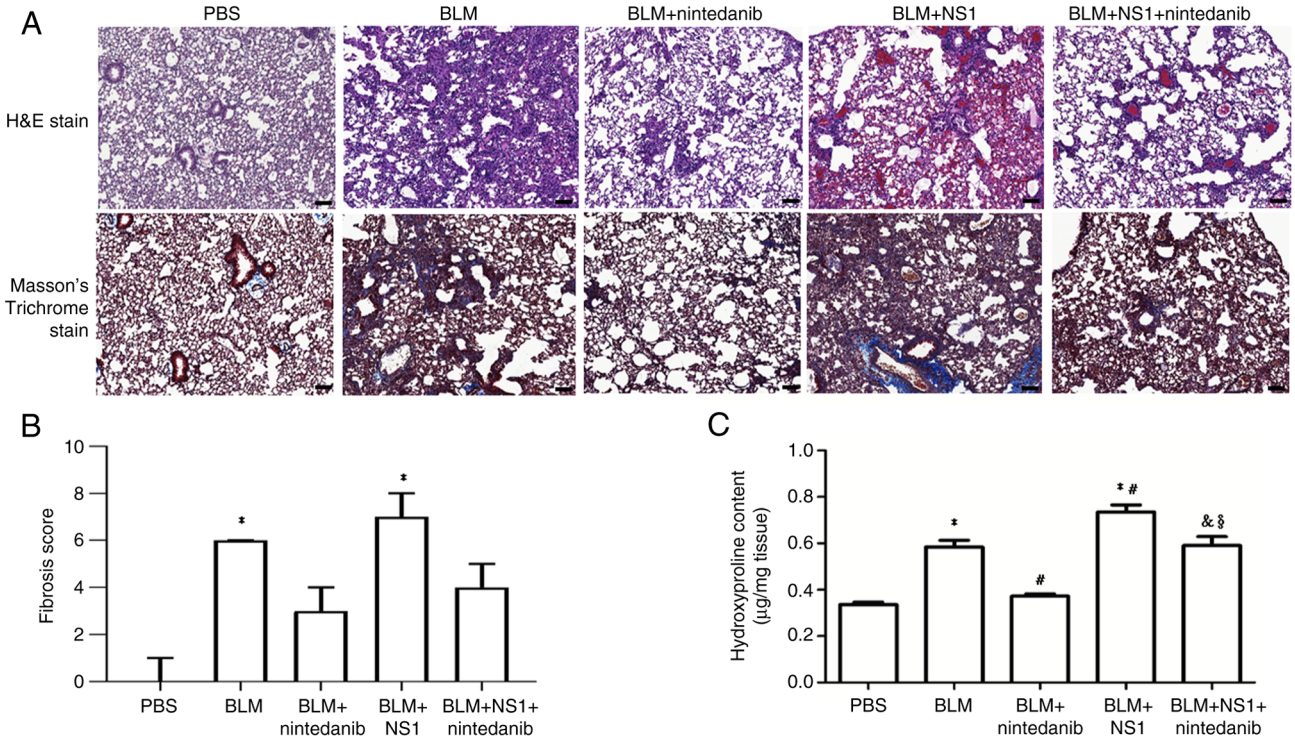

Figure 3. Histological staining of the lung tissues of mice. (A) Representative images of H&E and Masson's trichrome-stained mouse lung sections. Scale bar, 100 μm. Quantified result of (B) fibrosis score (BLM vs. PBS, P<0.05; BLM + NS1 vs. PBS, P<0.001) and (C) hydroxyproline content (BLM vs. PBS, P<0.001; BLM + NS1 vs. PBS, P<0.001; BLM + nintedanib vs. BLM, P<0.001; BLM + NS1 vs. BLM, P= P=0.016; BLM + nintedanib + NS1 vs. BLM + NS1, P=0.036; BLM + NS1 + nintedanib vs. BLM + nintedanib, P=0.006). *P<0.05 vs. the PBS (Control) group, #P<0.05 vs. the BLM group, &P<0.05 vs. the BLM + NS1 group, and §P<0.05 vs. the BLM + nintedanib group. H&E, hematoxylin and eosin; BLM, bleomycin; NS1, nonstructural protein 1.

the BLM + nintedanib group (P=0.006) (Fig. 3C). Moreover, quantification of key fibrotic marker levels, including those of TGF-β and collagen I, revealed that compared with BLM treatment alone, B19V NS1 administration significantly exacerbated fibrosis (P=0.015 and P<0.001, respectively). Conversely, the administration of nintedanib reduced the levels of these markers in mice from both the BLM and the BLM + NS1 groups (Fig. 4A-C; TGF-β: BLM vs. PBS, P<0.001; BLM + NS1 vs. PBS, P<0.001; BLM + nintedanib vs. BLM, P=0.001; BLM + nintedanib + NS1 vs. BLM + NS1, P<0.001; collagen I: BLM vs. PBS, P=0.019; BLM + NS1 vs. PBS, P<0.001; BLM + nintedanib vs. BLM, P=0.024; and BLM + nintedanib + NS1 vs. BLM + NS1, P<0.001).

B19V NS1 administration increases neutrophil and inflammasome involvement in the lungs of mice with BLM-induced pulmonary fibrosis. To confirm the involvement of neutrophils in the lungs of mice with BLM-induced pulmonary fibrosis treated with B19V NS1, levels of key neutrophil-related markers, including Cit-H3 and MPO, were determined. Significantly elevated Cit-H3 (P<0.001 and P<0.001, respectively) and MPO (P=0.001 and P<0.001, respectively) expression was detected in lung sections from mice in the BLM and BLM + NS1 groups compared with those from the PBS group (Fig. 5A-C), reflecting heightened neutrophil responses. Conversely, nintedanib treatment significantly reduced the levels of Cit-H3 (P=0.013 and P<0.001, respectively) and MPO (P=0.001 and P<0.001, respectively) compared with those in the BLM and BLM + NS1 groups. However, significantly more MPO-positive signals were detected in the BLM + NS1 + nintedanib group than in the BLM + nintedanib group (P=0.015; Fig. 5C). Additionally, the expression of inflammasome signaling factors, including IL-18 and IL-17A, significantly increased in the lungs of mice in the BLM and BLM + NS1 groups compared with those in the control group (IL-18: P<0.001 and P<0.001; IL-17A: P<0.001 and P<0.001, respectively; Fig. 5D and E). Significantly reduced levels of IL-18 and IL-17A were observed in the lung tissues of mice from both the BLM + nintedanib and the BLM + NS1 + nintedanib groups (Fig. 5D and E; IL-18: BLM + nintedanib vs. BLM, P=0.043; BLM + nintedanib + NS1 vs. BLM + NS1, P<0.001; IL-17A: BLM + nintedanib vs. BLM, P<0.03; BLM + nintedanib + NS1 vs. BLM + NS1; P<0.001).

Discussion

The present study revealed for the first time that B19V NS1 significantly exacerbates BLM-induced pulmonary fibrosis in mice by increasing inflammation and fibrosis, mainly through inflammasome activation and neutrophil-driven responses. Conversely, the administration of nintedanib reduced the expression of key fibrotic markers, such as IL-18, IL-17A, Cit-H3, and MPO, suggesting the therapeutic potential of nintedanib in exacerbating lung fibrosis associated with B19V NS1. In addition, there were significant differences in the proportions of B19V infection and hypertension between CTD patients with and without ILD. These findings revealed a mechanistic link between B19V infection and ILD, indicating that B19V, through NS1, acts as a potent exacerbator

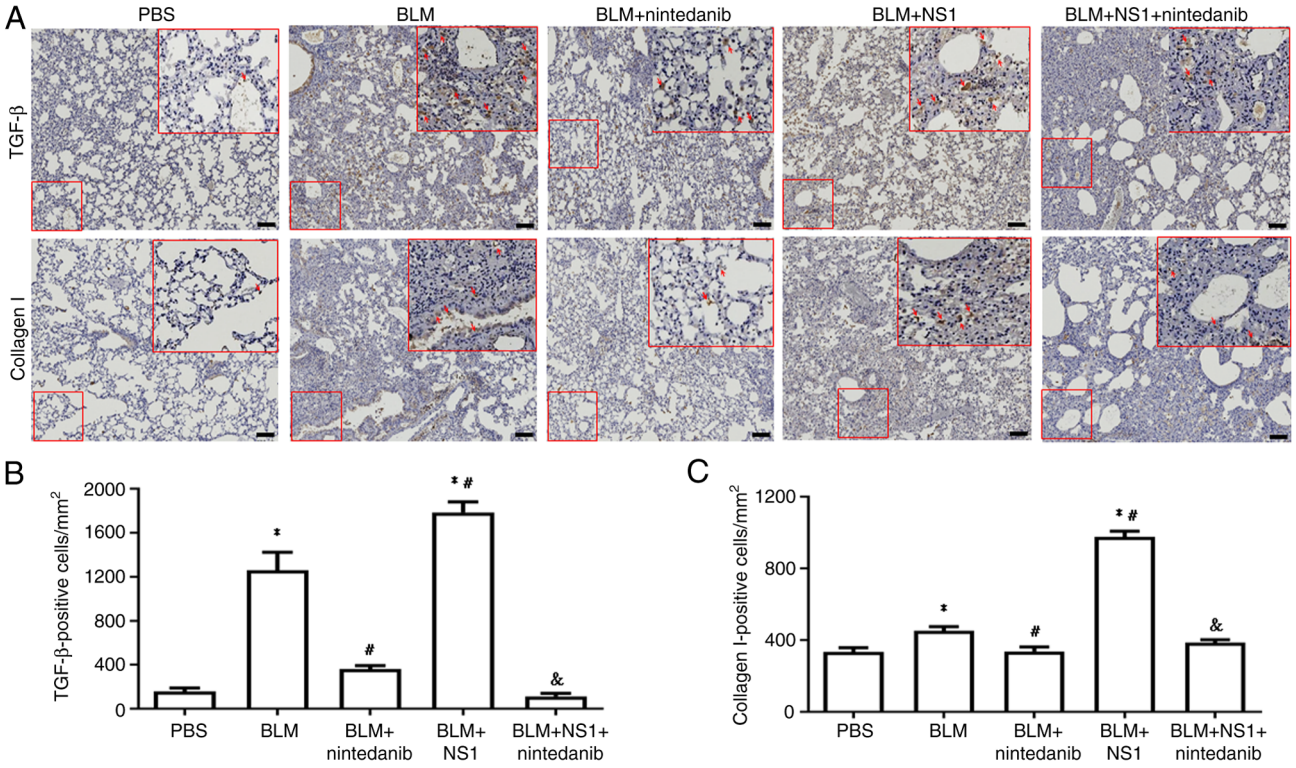

Figure 4. IHC staining of lung tissue of mice. (A) Representative images of lung sections of mice stained with TGF-β and collagen I. Scale bar, 100 μm. Quantified results of (B) TGF-β (BLM vs. PBS, P<0.001; BLM + NS1 vs. PBS, P<0.001; BLM + nintedanib vs. BLM, P=0.001; BLM + NS1 vs. BLM, P=0.015; BLM + nintedanib + NS1 vs. BLM + NS1, P<0.001) and (C) collagen I positive cells (BLM vs. PBS, P=0.019; BLM + NS1 vs. PBS, P<0.001; BLM + nintedanib vs. BLM, P=0.024; BLM + NS1 vs. BLM, P<0.001; BLM + nintedanib + NS1 vs. BLM + NS1, P<0.001) in lung sections of mice. *P<0.05 vs. the PBS (Control) group, #P<0.05 vs. the BLM group, and &P<0.05 vs. the BLM + NS1 group. IHC, immunohistochemistry; TGF transforming growth factor; BLM, bleomycin; NS1, nonstructural protein 1.

of ILD, further aggravating fibrosis in patients with already compromised pulmonary conditions.

Bleomycin induces fibrosis primarily through reactive oxygen species (ROS)-mediated oxidative stress, which triggers epithelial apoptosis, activates fibroblasts and promotes collagen deposition (32). ROS also activate the NLRP3 inflammasome, promoting fibrosis via the IL-1β/IL-1R/MyD88/NF-κB pathway and caspase-1-mediated activation of IL-1β and IL-18 (33-37). These findings are consistent with previous reports showing that B19V NS1 induces IL-6 and TGF-β expression and activates fibroblasts (21,23,38-40). In the present study, compared with BLM alone, combined treatment with BLM and B19V NS1 resulted in higher levels of inflammasome-related cytokines and collagen deposition. These findings provided a possible explanation for why B19V NS1 exacerbates BLM-induced pulmonary fibrosis. However, further studies are needed to clarify the precise role of B19V NS1 in ILD aggravation.

In a mouse model of BLM-induced fibrosis, neutrophil recruitment driven by chemokines such as CXCR2 contributes to tissue damage and fibrosis through the release of NETs, proinflammatory cytokines, and neutrophil elastase (41-43). Although evidence for B19V NS1-induced NET formation is limited, studies on dengue and Zika virus NS1 proteins have demonstrated their ability to promote NET release through platelet activation and neutrophil infiltration (44,45). In the present study, B19V NS1 exacerbated lung fibrosis through mechanisms that parallel those of BLM, including neutrophil-driven responses. The elevated levels of neutrophil markers, such as Cit-H3 and MPO, in the lung tissues of mice treated with both BLM and B19V NS1 indicated a strong correlation with increased neutrophil invasion, contributing to the chronic tissue damage characteristic of BLM-induced fibrosis.

Progressive fibrosing ILD poses a significant clinical challenge, as conventional treatments for pulmonary fibrosis often yield poor outcomes and only manage symptoms (12). nintedanib, a tyrosine kinase inhibitor targeting platelet-derived growth factor receptor, fibroblast growth factor receptor and vascular endothelial growth factor receptor, exerts antifibrotic and antiangiogenic effects and is approved by the United States Food and Drug Administration for treating IPF and SSc-associated ILD (46-48). In the current study, MPO and hydroxyproline levels remained increased in the BLM + NS1 + nintedanib group. Although nintedanib treatment mitigated several inflammatory and fibrotic responses exacerbated by NS1 in the BLM model, it did not fully reverse all pathological changes. These findings suggested that nintedanib only partly alleviates NS1-exacerbated lung injury and that its efficacy may be limited in the presence of NS1-mediated fibrosis. Further studies are needed to explore combination strategies or alternative treatments that more effectively counteract NS1-driven fibrotic pathways.

Notably, the present study has several limitations that should be acknowledged. First, the sample size was relatively small, particularly in the subgroup of CTD patients

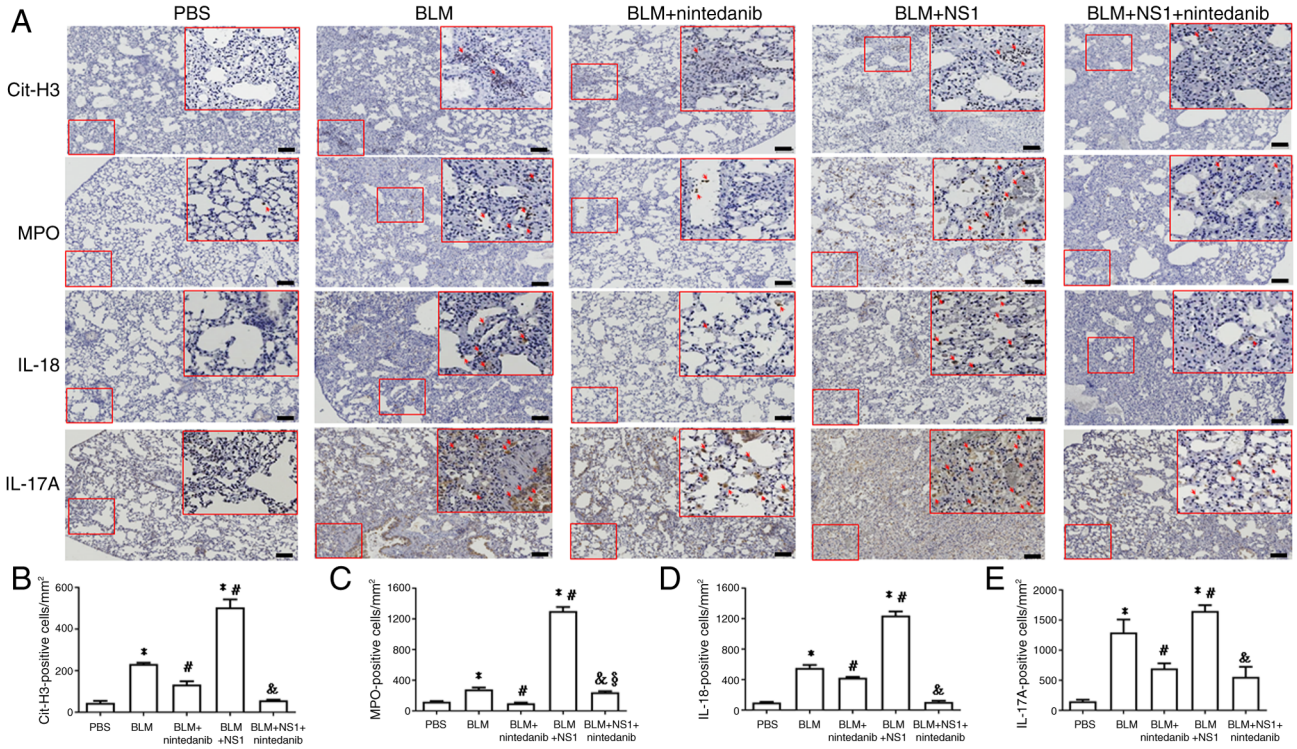

Figure 5. Expressions of neutrophil-related and inflammasome markers. (A) Representative immunohistochemistry images of the lung section of mice stained with (A) Cit-H3, MPO, IL-18 and IL-17. Scale bar, 100 μm. Quantification of (B) Cit-H3 (BLM vs. PBS, P<0.001; BLM + NS1 vs. PBS, P<0.001; BLM + nintedanib vs. BLM, P=0.013; BLM + NS1 vs. BLM, P<0.001; BLM + nintedanib + NS1 vs. BLM + NS1, P<0.001), (C) MPO (BLM vs. PBS, P=0.001; BLM + NS1 vs. PBS, P<0.001; BLM + nintedanib vs. BLM, P<0.001; BLM + NS1 vs. BLM, P= P<0.001; BLM + nintedanib + NS1 vs. BLM + NS1, P<0.001; BLM + nintedanib + NS1 vs. BLM + nintedanib, P=0.015), (D) IL-18 (BLM vs. PBS, P<0.001; BLM + NS1 vs. PBS, P<0.001; BLM + nintedanib vs. BLM, P=0.043; BLM + NS1 vs. BLM, P<0.001; BLM + nintedanib + NS1 vs. BLM + NS1, P<0.001), and (E) IL-17 (BLM vs. PBS, P<0.001; BLM + NS1 vs. PBS, P<0.001; BLM + nintedanib vs. BLM, P<0.03; BLM + NS1 vs. BLM, P<0.001; BLM + nintedanib + NS1 vs. BLM + NS1, P<0.001) positive cells in lung sections of mice. *P<0.05 vs. the PBS (Control) group, #P<0.05 vs. the BLM group, &P<0.05 vs. the BLM + NS1 group, and §P<0.05 vs. the BLM + nintedanib group. Cit-H3, citrullinated histone H3; MPO, myeloperoxidase; IL, interleukin; BLM, bleomycin; NS1, nonstructural protein 1.

with ILD (n=33), which may limit the statistical power and generalizability of the findings. These factors may influence disease severity and outcomes, and their absence could have introduced residual confounding. Therefore, the results should be interpreted with caution and further studies with larger, well-characterized cohorts are needed to confirm these findings in the future. Second, a group receiving NS1 treatment alone was not included in the present study. While the primary objective was to investigate the effect of NS1 in the context of BLM-induced lung injury, the lack of an NS1-only control group made it difficult to fully determine whether NS1 itself can independently induce fibrotic changes in the lungs. Including such a group would help clarify whether the observed effects are specific to the interaction between NS1 and BLM-induced injury or partially attributable to NS1 alone. Therefore, future studies should incorporate an NS1-only group to delineate the individual more precisely and combined effects of NS1 and BLM on the progression of pulmonary fibrosis. Third, direct mechanistic evidence to confirm the causal role of neutrophil activation and inflammasome signaling in the NS1-induced exacerbation of fibrosis was lacking. While the findings suggested that NS1 may promote pulmonary fibrosis through enhanced neutrophil activity and activation of the NLRP3 inflammasome pathway, these conclusions are based on correlative data. The absence of experiments employing specific inhibitors, such as NLRP3 or NETosis inhibitors, limits the ability of the present study to definitively establish causality. Therefore, future studies incorporating targeted inhibition or loss-of-function approaches are needed to validate these mechanistic links and strengthen the causal interpretation of our findings. Finally, a key limitation is that the experiments were conducted in mouse models, which may not fully replicate the complex pathophysiology of human disease. Consequently, the findings and therapeutic effects observed here may not directly translate to humans due to species-specific differences in immune responses, disease progression, and drug metabolism (49). Therefore, further validation in clinical settings or human-derived models is necessary to confirm the relevance of these results to human patients.

Overall, the results of the current study provided a clinical and mechanistic connection between B19V infection and the progression of pulmonary fibrosis. The clinical data indicated a higher incidence of B19V infection among CTD patients with ILD, suggesting a potential association with the development of ILD. Experimental findings further demonstrated that B19V, through its NS1 protein, may exacerbate ILD and worsen fibrosis in patients already affected by lung conditions, particularly by activating the inflammasome and driving neutrophil responses. These findings build on previous evidence of B19V in ILD patients, reinforcing the possible role of B19V NS1 in exacerbating fibrogenesis.

Acknowledgements

Not applicable.

Funding

The present study was supported by grants from the National Science and Technology Council (grant no. NSTC 112-2314-B040-015) and Chung Shan Medical University (grant no. CSMU-INT-113-04). The funders had no role in the study design, data collection and analysis, the decision to publish, or the preparation of the manuscript.

Availability of data and materials

The data generated in the present study may be requested from the corresponding author.

Author's contribution

TCH, CCT, DYC and BST were involved in the study conception and design, drafting and revising of the manuscript and data analysis. CWK and ZHW performed the experiments and analyzed the data. TCH, DYC and BST confirm the authenticity of all the raw data. All authors read and approved the final manuscript.

Ethics approval and consent to participate

The China Medical University Hospital's Institutional Review Board approved the study (IRB approval number CMUH110-REC2-178), and all participants provided written informed consent following the Declaration of Helsinki's ethical guidelines for medical research involving human subjects. The animal study protocol was approved by the Institutional Animal Care and Use Committee of Chung Shan Medical University, Taiwan (approval numbers 2803 and 112065).

Patient consent for publication

Not applicable.

Competing interests

The authors declare that they have no competing interests.

References

1. Cottin V, Wollin L, Fischer A, Quaresma M, Stowasser S and Harari S: Fibrosing interstitial lung diseases: knowns and unknowns. Eur Respir Rev 28: 180100, 2019.
2. Podolanczuk AJ, Thomson CC, Remy-Jardin M, Richeldi L, Martinez FJ, Kolb M and Raghu G: Idiopathic pulmonary fibrosis: State of the art for 2023. Eur Respir J 61: 2200957, 2023.
3. Matson SM and Demoruelle MK: Connective tissue disease-associated interstitial lung disease. Rheum Dis Clin North Am 50: 423-438, 2024.
4. Wan Q, Zhang X, Zhou D, Xie R, Cai Y, Zhang K and Sun X: Inhaled nano-based therapeutics for pulmonary fibrosis: Recent advances and future prospects. J Nanobiotechnology 21: 215, 2023.
5. Andersson-Sjöland A, de Alba CG, Nihlberg K, Becerril C, Ramírez R, Pardo A, Westergren-Thorsson G and Selman M: Fibrocytes are a potential source of lung fibroblasts in idiopathic pulmonary fibrosis. Int J Biochem Cell Biol 40: 2129-2140, 2008.
6. Al Oweidat KS, Abdulelah AA, Toubasi AA, Abdulelah M, Alatteili NZ and Abdulelah ZA: The clinical efficacy and safety of nintedanib in the treatment of interstitial lung disease among patients with systemic sclerosis: Systematic review. Can Respir J 2025: 1682546, 2025.
7. Qiu J, Söderlund-Venermo M and Young NS: Human parvoviruses. Clin Microbiol Rev 30: 43-113, 2017.
8. Arvia R, Stincarelli MA, Manaresi E, Gallinella G and Zakrzewska K: Parvovirus B19 in rheumatic diseases. Microorganisms 12: 1708, 2024.
9. Tzang CC, Chi LY, Lee CY, Chang ZY, Luo CA, Chen YH, Lin TA, Yu LC, Chen YR, Tzang BS and Hsu TC: Clinical implications of human Parvovirus B19 infection on autoimmunity and autoimmune diseases. Int Immunopharmacol 147: 113960, 2025.
10. Janner D, Bork J, Baum M and Chinnock R: Severe pneumonia after heart transplantation as a result of human parvovirus B19. J Heart Lung Transplant 13: 336-338, 1994.
11. Bousvaros A, Sundel R, Thorne GM, McIntosh K, Cohen M, Erdman DD, Perez-Atayde A, Finkel TH and Colin AA: Parvovirus B19-associated interstitial lung disease, hepatitis, and myositis. Pediatr Pulmonol 26: 365-369, 1998.
12. Atzeni F, Alciati A, Gozza F, Masala IF, Siragusano C and Pipitone N: Interstitial lung disease in rheumatic diseases: an update of the 2018 review. Expert Rev Clin Immunol 21: 209-226, 2025.
13. Nikkari S, Mertsola J, Korvenranta H, Vainionpää R and Toivanen P: Wegener's granulomatosis and parvovirus B19 infection. Arthritis Rheum 37: 1707-1710, 1994.
14. Magro CM, Crowson AN, Dawood M and Nuovo GJ: Parvoviral infection of endothelial cells and its possible role in vasculitis and autoimmune diseases. J Rheumatol 29: 1227-1235, 2002.
15. Magro CM, Nuovo G, Ferri C, Crowson AN, Giuggioli D and Sebastiani M: Parvoviral infection of endothelial cells and stromal fibroblasts: A possible pathogenetic role in scleroderma. J Cutan Pathol 31: 43-50, 2004.
16. Magro CM, Allen J, Pope-Harman A, Waldman WJ, Moh P, Rothrauff S and Ross P Jr: The role of microvascular injury in the evolution of idiopathic pulmonary fibrosis. Am J Clin Pathol 119: 556-567, 2003.
17. Li X, Chen X and Zhang Y: Interstitial pneumonia with pulmonary parvovirus B19 infection. Med Clin (Barc) 159: e17-e18, 2022.
18. Magro CM, Wusirika R, Frambach GE, Nuovo GJ, Ferri C and Ross P Jr: Autoimmune-like pulmonary disease in association with parvovirus B19: A clinical, morphologic, and molecular study of 12 cases. Appl Immunohistochem Mol Morphol 14: 208-216, 2006.
19. Moffatt S, Tanaka N, Tada K, Nose M, Nakamura M, Muraoka O, Hirano T and Sugamura K: A cytotoxic nonstructural protein, NS1, of human parvovirus B19 induces activation of interleukin-6 gene expression. J Virol 70: 8485-8491, 1996.
20. Hsu TC, Tzang BS, Huang CN, Lee YJ, Liu GY, Chen MC and Tsay GJ: Increased expression and secretion of interleukin-6 in human parvovirus B19 non-structural protein (NS1) transfected COS-7 epithelial cells. Clin Exp Immunol 144: 152-157, 2006.
21. Martinović Kaliterna D and Petrić M: Biomarkers of skin and lung fibrosis in systemic sclerosis. Expert Rev Clin Immunol 15: 1215-1223, 2019.
22. Dsouza NN, Alampady V, Baby K, Maity S, Byregowda BH and Nayak Y: Thalidomide interaction with inflammation in idiopathic pulmonary fibrosis. Inflammopharmacology 31: 1167-1182, 2023.
23. Arvia R, Margheri F, Stincarelli MA, Laurenzana A, Fibbi G, Gallinella G, Ferri C, Del Rosso M and Zakrzewska K: Parvovirus B19 activates in vitro normal human dermal fibroblasts: A possible implication in skin fibrosis and systemic sclerosis. Rheumatology (Oxford) 59: 3526-3532, 2020.
24. Jeganathan N and Sathananthan M: Connective tissue disease-related interstitial lung disease: Prevalence, patterns, predictors, prognosis, and treatment. Lung 198: 735-759, 2020.
25. Smith RE, Strieter RM, Phan SH, Lukacs NW, Huffnagle GB, Wilke CA, Burdick MD, Lincoln P, Evanoff H and Kunkel SL: Production and function of murine macrophage inflammatory protein-1 alpha in bleomycin-induced lung injury. J Immunol 153: 4704-4712, 1994.
26. Maher TM, Wells AU and Laurent GJ: Idiopathic pulmonary fibrosis: Multiple causes and multiple mechanisms? Eur Respir J 30: 835-839, 2007.
27. Mor A, Segal Salto M, Katav A, Barashi N, Edelshtein V, Manetti M, Levi Y, George J and Matucci-Cerinic M: Blockade of CCL24 with a monoclonal antibody ameliorates experimental dermal and pulmonary fibrosis. Ann Rheum Dis 78: 1260-1268, 2019.

28. Chiang SR, Lin CY, Chen DY, Tsai HF, Lin XC, Hsu TC and Tzang BS: The effects of human parvovirus VP1 unique region in a mouse model of allergic asthma. PLoS One 14: e0216799, 2019.
29. Ishikawa Y, Iwata S, Hanami K, Nawata A, Zhang M, Yamagata K, Hirata S, Sakata K, Todoroki Y, Nakano K, *et al*: Relevance of interferon-gamma in pathogenesis of life-threatening rapidly progressive interstitial lung disease in patients with dermatomyositis. Arthritis Res Ther 20: 240, 2018.
30. Tzang CC, Lin WC, Huang ES, Kang YF, Cheng YH, Tzang BS and Hsu TC: Interstitial lung disease biomarkers: A systematic review and meta-analysis. Clin Chim Acta 577: 120473, 2025.
31. Hübner RH, Gitter W, El Mokhtari NE, Mathiak M, Both M, Bolte H, Freitag-Wolf S and Bewig B: Standardized quantification of pulmonary fibrosis in histological samples. Biotechniques 44: 507-511, 514-517, 2008.
32. Mohammed SM, Al-Saedi HFS, Mohammed AQ, Amir AA, Radi UK, Sattar R, Ahmad I, Ramadan MF, Alshahrani MY, Balasim HM and Alawadi A: Mechanisms of bleomycin-induced lung fibrosis: A review of therapeutic targets and approaches. Cell Biochem Biophys 82: 1845-1870, 2024.
33. Song C, He L, Zhang J, Ma H, Yuan X, Hu G, Tao L, Zhang J and Meng J: Fluorofenidone attenuates pulmonary inflammation and fibrosis via inhibiting the activation of NALP3 inflammasome and IL-1β/IL-1R1/MyD88/NF-κB pathway. J Cell Mol Med 20: 2064-2077, 2016.
34. Jegal Y, Kim DS, Shim TS, Lim CM, Do Lee S, Koh Y, Kim WS, Kim WD, Lee JS, Travis WD, *et al*: Physiology is a stronger predictor of survival than pathology in fibrotic interstitial pneumonia. Am J Respir Crit Care Med 171: 639-644, 2005.
35. Artlett CM, Sassi-Gaha S, Hope JL, Feghali-Bostwick CA and Katsikis PD: Mir-155 is overexpressed in systemic sclerosis fibroblasts and is required for NLRP3 inflammasome-mediated collagen synthesis during fibrosis. Arthritis Res Ther 19: 144, 2017.
36. Zhang WJ, Chen SJ, Zhou SC, Wu SZ and Wang H: Inflammasomes and fibrosis. Front Immunol 12: 643149, 2021.
37. Colunga Biancatelli RML, Solopov PA and Catravas JD: The Inflammasome NLR family pyrin domain-containing protein 3 (NLRP3) as a novel therapeutic target for idiopathic pulmonary fibrosis. Am J Pathol 192: 837-846, 2022.
38. Hsu TC, Tsai CC, Chiu CC, Hsu JD and Tzang BS: Exacerbating effects of human parvovirus B19 NS1 on liver fibrosis in NZB/W F1 mice. PLoS One 8: e68393, 2013.
39. Arvia R, Zakrzewska K, Giovannelli L, Ristori S, Frediani E, Del Rosso M, Mocali A, Stincarelli MA, Laurenzana A, Fibbi G and Margheri F: Parvovirus B19 induces cellular senescence in human dermal fibroblasts: Putative role in systemic sclerosis-associated fibrosis. Rheumatology (Oxford) 61: 3864-3874, 2022.
40. Huang CL, Chen DY, Tzang CC, Lin JW, Tzang BS and Hsu TC: Celastrol attenuates human parvovirus B19 NS1-induced NLRP3 inflammasome activation in macrophages. Mol Med Rep 28: 193, 2023.
41. Suzuki M, Ikari J, Anazawa R, Tanaka N, Katsumata Y, Shimada A, Suzuki E and Tatsumi K: PAD4 deficiency improves bleomycin-induced neutrophil extracellular traps and fibrosis in mouse lung. Am J Respir Cell Mol Biol 63: 806-818, 2020.
42. Chen WC, Chen NJ, Chen HP, Yu WK, Su VY, Chen H, Wu HH and Yang KY: Nintedanib reduces neutrophil chemotaxis via activating GRK2 in bleomycin-induced pulmonary fibrosis. Int J Mol Sci 21: 4735, 2020.
43. Cheng IY, Liu CC, Lin JH, Hsu TW, Hsu JW, Li AF, Ho WC, Hung SC and Hsu HS: Particulate matter increases the severity of bleomycin-induced pulmonary fibrosis through KC-mediated neutrophil chemotaxis. Int J Mol Sci 21: 227, 2019.
44. Garishah FM, Rother N, Riswari SF, Alisjahbana B, Overheul GJ, van Rij RP, van der Ven A, van der Vlag J and de Mast Q: Neutrophil extracellular traps in dengue are mainly generated NOX-independently. Front Immunol 12: 629167, 2021.
45. de Siqueira Santos R, Rochael NC, Mattos TRF, Fallett E, Silva MF, Linhares-Lacerda L, de Oliveira LT, Cunha MS, Mohana-Borges R, Gomes TA, *et al*: Peripheral nervous system is injured by neutrophil extracellular traps (NETs) elicited by nonstructural (NS) protein-1 from Zika virus. FASEB J 37: e23126, 2023.
46. Ghazipura M, Mammen MJ, Herman DD, Hon SM, Bissell BD, Macrea M, Kheir F, Khor YH, Knight SL, Raghu G, *et al*: Nintedanib in progressive pulmonary fibrosis: A systematic review and meta-analysis. Ann Am Thorac Soc 19: 1040-1049, 2022.
47. Singh P, Thampi G, Gupta K, Gangte N, Pattnaik B, Agrawal A and Kukreti R: Clinical efficacy and safety evaluation of drug therapies for the treatment of progressive fibrotic-interstitial lung diseases (PF-ILDs): A network meta-analysis of randomized controlled trials. Expert Rev Clin Immunol 21: 1135-1170, 2025.
48. Srivali N, De Giacomi F, Moua T and Ryu JH: Perioperative antifibrotic therapy for patients with idiopathic pulmonary fibrosis undergoing lung cancer surgery: A systematic review and meta-analysis. Heart Lung 74: 266-275, 2025.
49. Tang Z, Yang H, Liang X, Chen J, He Q, Zhu D and Liu Y: Animal models for connective tissue disease-associated interstitial lung disease: Current status and future directions. Autoimmun Rev 24: 103919, 2025.